# Antibiotic-induced degradation of FtsZ reveals distinct stages of *Bacillus subtilis* FtsZ ring assembly and constriction

Nadine Silber[1§], Christian Mayer[1§], Cruz L Matos de Opitz[1], Peter Sass[1,2*]

[1]Department of Microbial Bioactive Compounds, Interfaculty Institute of Microbiology and Infection Medicine, University of Tübingen, Auf der Morgenstelle 28, 72076 Tübingen, Germany

[2]Cluster of Excellence - Controlling Microbes to Fight Infections, 72076 Tübingen, Germany

[§] shared first author

[*]Correspondence should be addressed to Peter Sass (peter.sass@uni-tuebingen.de)

Running title: Distinct stages of FtsZ ring assembly and constriction

Keywords: cytokinesis, cell division, guanosine nucleotides, FtsZ treadmilling, ADEP

**Abstract**

ADEP antibiotics induce the degradation of the cell division protein FtsZ, thereby primarily depleting the cytoplasmic FtsZ pool that is needed for treadmilling FtsZ rings. We here studied the effect of ADEP on FtsZ ring formation. Our data reveal the disintegration of early FtsZ rings during ADEP treatment, while progressed FtsZ rings finalize cytokinesis, thus indicating different roles for FtsZ treadmilling during distinct stages of divisome assembly and constriction.

**Main**

Bacterial cell division is a vital process in most bacteria and ensures the generation of progeny, usually by yielding equal daughter cells. In rod-shaped bacteria, such as *Bacillus subtilis*, cell division occurs at midcell, driven by FtsZ and orchestrated by a diverse set of proteins together constituting the divisome[1,2]. As the pacemaker of cell division, FtsZ self-polymerizes into protofilaments, which are characterized by additional lateral interactions to support protofilament bundling and producing higher order polymer assemblies[3], and finally builds the FtsZ ring at the future division site. Here, the FtsZ ring acts as the scaffold for other divisome members. During polymerization, the T7 loop of one FtsZ subunit inserts into the GTP binding site of the next subunit thereby triggering hydrolysis of GTP to GDP[4,5]. This favors the disassembly of FtsZ protofilaments resulting in a constant exchange of FtsZ subunits between the FtsZ ring and the cytoplasmic pool of FtsZ monomers. As the cell cycle proceeds, the divisome constricts and synthesizes septal peptidoglycan to allow for septum formation and eventually cytokinesis. Over the last years, principally two mechanisms have been discussed on how the force required for cytokinesis is generated, either by the chemical energy of FtsZ-dependent GTP hydrolysis[6,7], or alternatively by peptidoglycan synthesis[6,8]. Recently, FtsZ treadmilling, the GTP-dependent dynamic exchange of FtsZ from the cytoplasmic pool with the FtsZ ring, has been reported to drive divisome progression and constriction in *B. subtilis*[9]. In *Staphylococcus aureus*, this process may occur via two steps,

an initial step involving FtsZ treadmilling and a second step which increasingly depends on peptidoglycan synthesis[10].

To investigate the role of treadmilling in *B. subtilis* FtsZ ring formation further, we employed antibiotics of the ADEP class as tools to modulate the cytoplasmic pool of FtsZ. ADEP deregulates the bacterial caseinolytic protease, activating its dormant core ClpP for the untimely degradation of FtsZ[11,12]. ADEP incubation thus leads to an impressive filamentation phenotype of *B. subtilis* at concentrations close to the minimal inhibitory concentration (MIC)[12,13]. Very recently, we showed that ADEP-ClpP preferably targets the N terminus of monomeric FtsZ, leading to unfolding and degradation of the FtsZ N-terminal domain[14]. Intriguingly, N-terminal degradation was prevented upon nucleotide binding to FtsZ, most probably due to a stabilization of the FtsZ protein fold. Therefore, at ADEP concentrations resulting in a filamentation phenotype, ADEP primarily leads to a depletion of the cytoplasmic pool of nucleotide-free FtsZ in the bacterial cell[14], thus reducing the FtsZ concentration below the critical level needed for FtsZ ring formation[15,16] and continuously sequestering available FtsZ needed for treadmilling (Fig. 1a). Hence, ADEP is instrumental to investigate the role of the cytoplasmic FtsZ pool and treadmilling in FtsZ ring formation and dynamics. To do so, we first tested the effect of ADEP on polymerized FtsZ (in the presence of GTP) (Fig. 1b). Once assembled into protofilaments, FtsZ substantially resisted the degradation by ADEP-ClpP. It may thus be hypothesized that, if FtsZ ring assembly and constriction fully depend on FtsZ treadmilling, ADEP treatment should result in the disintegration of early as well as late stage FtsZ rings, or at least, the progression of late stage FtsZ rings should be halted. To test this hypothesis, we conducted time-lapse fluorescence and super-resolution microscopy experiments with ADEP-treated *B. subtilis* strain 2020, which expresses FtsZ fused to GFP using filamentation concentrations of the antibiotic. By following FtsZ ring formation over time, we observed that ADEP inhibited the initiation of FtsZ ring assembly, and early FtsZ rings that had just been formed disintegrated. In contrast, more progressed FtsZ rings constricted and finished septum formation, apparently being unaffected by ADEP treatment, finally yielding two separated

daughter cells (Fig. 1cd, Supplementary Fig. S1 and S2). Following up on this, we investigated whether the arrival of the late-stage cell division protein PBP2b[17], a septal peptidoglycan synthase, would coincide with a successful constriction of progressed FtsZ rings during ADEP-treatment. By using *B. subtilis* strain CM03, which allows for the concomitant expression of mCherry-FtsZ and GFP-PBP2b, we observed that the divisome consistently finalized cell division after PBP2b had substantially arrived at the septum area and had formed clear foci. Contrariwise, earlier FtsZ rings disintegrated prior to the observed arrival of PBP2b (Fig. 1e, Supplementary Fig. S3). Hence, our data imply distinct stages during FtsZ ring initiation, maturation and constriction. Obviously, during ADEP treatment it is distinguished between early and more progressed FtsZ rings, thereby adding another level of complexity to the elaborate mechanism of ADEP action. Also, our data suggest a two-step model of cell division in *B. subtilis* (Fig. 2), in which more progressed FtsZ rings are significantly less sensitive to a depletion of the cytoplasmic pool of nucleotide-free FtsZ, and thus less dependent on FtsZ treadmilling, in contrast to initial assembly and early stage FtsZ rings.

## Methods

### Protein purification

FtsZ and ClpP proteins were derived of *B. subtilis* 168 (*trpC2*; wild-type strain; NC_000964.3) and were expressed as C-terminally $His_6$-tagged proteins in *E. coli* BL21(DE3) harboring the respective expression plasmid as described earlier[12]. Quantity and quality of the purified proteins were verified by Bradford assay (using bovine serum albumin as control), Nanodrop spectrophotometry (Nanodrop Technologies) and SDS-PAGE. We have shown previously that purification-tags have no effect on FtsZ degradation or enzyme activity of both proteins[14].

### *In vitro* FtsZ polymerization and degradation assays

For GTP-dependent polymerization *in vitro*, purified *B. subtilis* 168 FtsZ (25 µM) was preincubated in polymerization buffer (50 mM MES/NaOH, pH 6.5, 50 mM KCl, 10 mM $MgCl_2$) for 10 min on ice. After initial incubation for 4 min at 37 °C allowing baseline correction, GTP was added to the

respective reaction mixture to a final concentration of 1 mM. Then, reaction mixtures were transferred into a photometer cuvette for monitoring light transmission at 400 nm and 37 °C over time. For *in vitro* degradation of polymerized FtsZ, 12 µM ADEP2 (or equal volume of DMSO as a control) and 1.5 µM purified ClpP protein (monomer concentration) were added to the polymerization reaction after 16 min, as indicated, and light transmission was further monitored for 34 min. As an independent control, FtsZ (4 µM) was incubated with 1 mM GTP in activity buffer (50 mM Tris/HCl pH 8, 25 mM $MgCl_2$, 100 mM KCl, 2 mM DTT) at 37 °C for 30 min. Then 1.5 µM ClpP (monomer concentration) and 3.75 µM ADEP (or equal volume of DMSO as a control) were added to the reaction mixtures that were further incubated at 37 °C. Samples were taken after 120 min and were analyzed via SDS-PAGE using standard techniques as previously described[12,14].

**Cloning strategy**

For colocalization studies of FtsZ with PBP2b (mCherry-FtsZ/GFP-PBP2b), strain *B. subtilis* CM03 was constructed as follows. Plasmid pJCM02 was generated using the coding sequence of *pbpB* that was amplified from chromosomal DNA of *B. subtilis* 168 (*trpC2*; wild-type strain; NC_000964.3) *via* PCR using the following primers: oCM07 5'-GGAAGCGGCTCAGGCTCCCGGATCCACATTCAAATGCCAAAAAAGAATAAATTTATG-3', oCM08 5'-CGCGGCCGCTCTAGAACTAGAATTCTTAATCAGGATTTTTAAACTTAACCTTG-3'. The amplicon was then ligated into the linearized plasmid pJCM01[13] by a Gibson isothermal reaction. The resulting plasmid was transformed into *B. subtilis* CM01 (*trpC2 cat aprE::Pspac-mcherry-ftsZ*)[13] to give strain CM03 (*trpC2 cat aprE::Pspac-mcherry-ftsZ; spc amyE::Pxyl-msfgfp-pbpB*).

**Super-resolution and time-lapse fluorescence microscopy**

Cells of *B. subtilis* 2020 (*trpC2 spc amyE::Pxyl-gfp-ftsZ*)[18] or *B. subtilis* CM03 (*trpC2 cat aprE::Pspac-mcherry-ftsZ; spc amyE::Pxyl-msfgfp-pbpB*) were grown at 37 °C to early-exponential phase (optical density at 600 nm ($OD_{600}$) of 0.1). Then, cells were pre-incubated in

lysogeny broth (LB) supplemented with 0.125-0.25 µg/ml ADEP2 or DMSO as a control. Of note, the ADEP concentration used here results in filamentation of *B. subtilis*, resembling a phenotype that is mainly due to FtsZ degradation, whereas biomass increase and metabolism in general remain unaltered[12]. For the expression of GFP and mCherry fusion proteins, *Pxyl* and *Pspac* promoters were induced using 0.1-0.2% xylose and 0.1 mM IPTG, respectively. Bacteria were then transferred onto microscope slides covered with a thin film of 1.5% agarose in 25% LB containing 0.125-0.25 µg/ml ADEP2. Phase contrast and fluorescence images were taken at distinct time points as indicated. Super-resolution images were recorded using a Zeiss Axio Observer Z1 LSM800 equipped with an Airyscan detector and a C Plan-Apo 63x/1.4 Oil DIC objective (Zeiss, Germany). Images were processed using the ZEN2.3 image analysis software package (Zeiss). Time-lapse micrographs were obtained using a Nikon Eclipse Ti automated microscope equipped with a Perfect Focus system (Nikon Instruments Europe BV, Netherlands), an Orca Flash 4.0 camera (Hamamatsu, Photonics, Japan) and CFI Plan-Apo DM 100x/1.45 Oil Ph3 objective (Nikon). Image acquisition and analysis were performed via the NIS elements AR software package (Nikon).

**Acknowledgments**

We gratefully thank Heike Brötz-Oesterhelt for providing ADEP2, as well as Leendert Hamoen, Jeff Errington and Kürşad Turgay for the kind gift of strains and plasmids. We also thank Anne Berscheid for critically reading and discussing the manuscript.

N Silber, C Mayer, C Matos and P Sass performed and designed experiments, analyzed data and prepared figures. P Sass conceived and supervised the study and wrote the manuscript. All authors discussed data and edited the manuscript.

**Competing interests**

The authors have declared that no competing interests exist.

## Funding

The authors appreciate funding by the Deutsche Forschungsgemeinschaft (DFG, German Research Foundation): Project-ID 398967434 (TRR 261-A02) as well as support by infrastructural funding from the Cluster of Excellence EXC 2124 Controlling Microbes to Fight Infections.

## References

1 den Blaauwen, T., Hamoen, L. W. & Levin, P. A. The divisome at 25: the road ahead. *Curr Opin Microbiol* **36**, 85-94, (2017).

2 Silber, N., Matos, C., Mayer, C. & Sass, P. Cell division protein FtsZ: from structure and mechanism to antibiotic target. *Fut Microbiol*, DOI: 10.2217/fmb-2019-0348, in press, (2020).

3 Sundararajan, K. & Goley, E. D. The intrinsically disordered C-terminal linker of FtsZ regulates protofilament dynamics and superstructure *in vitro*. *J Biol Chem.* **292**, 20509-20527, (2017).

4 Scheffers, D. J., de Wit, J. G., den Blaauwen, T. & Driessen, A. J. GTP hydrolysis of cell division protein FtsZ: evidence that the active site is formed by the association of monomers. *Biochemistry* **41**, 521-529, (2002).

5 Scheffers, D. J. & Driessen, A. J. Immediate GTP hydrolysis upon FtsZ polymerization. *Mol Microbiol* **43**, 1517-1521, (2002).

6 Coltharp, C. & Xiao, J. Beyond force generation: Why is a dynamic ring of FtsZ polymers essential for bacterial cytokinesis? *Bioessays.* **39**, 1-11, (2017).

7 Li, Z., Trimble, M. J., Brun, Y. V. & Jensen, G. J. The structure of FtsZ filaments *in vivo* suggests a force-generating role in cell division. *Embo J* **26**, 4694-4708, (2007).

8 Coltharp, C., Buss, J., Plumer, T. M. & Xiao, J. Defining the rate-limiting processes of bacterial cytokinesis. *Proc Natl Acad Sci USA* **113**, E1044-1053, (2016).

9 Bisson-Filho, A. W. *et al.* Treadmilling by FtsZ filaments drives peptidoglycan synthesis and bacterial cell division. *Science* **355**, 739-743, (2017).

10 Monteiro, J. M. *et al.* Peptidoglycan synthesis drives an FtsZ-treadmilling-independent step of cytokinesis. *Nature* **554**, 528-532, (2018).

11 Brötz-Oesterhelt, H. *et al.* Dysregulation of bacterial proteolytic machinery by a new class of antibiotics. *Nat Med* **11**, 1082-1087, (2005).

12 Sass, P., Josten, M., Famulla, K., Schiffer, G., Sahl, H. G., Hamoen, L. & Brötz-Oesterhelt, H. Antibiotic acyldepsipeptides activate ClpP peptidase to degrade the cell division protein FtsZ. *Proc Natl Acad Sci USA* **108**, 17474-17479, (2011).

13 Mayer, C., Sass, P. & Brötz-Oesterhelt, H. Consequences of dosing and timing on the antibacterial effects of ADEP antibiotics. *Int J Med Microbiol* **309**, 151329, (2019).

14 Silber, N., Pan, S., Schäkermann, S., Mayer, C., Brötz-Oesterhelt, H. & Sass, P. Cell division protein FtsZ is unfolded for N-terminal degradation by antibiotic-activated ClpP. *mBio* **11**(3), e01006-20, (2020).

15 Huecas, S., Llorca, O., Boskovic, J., Martin-Benito, J., Valpuesta, J. M. & Andreu, J. M. Energetics and geometry of FtsZ polymers: nucleated self-assembly of single protofilaments. *Biophys J* **94**, 1796-1806, (2008).

16 Mukherjee, A. & Lutkenhaus, J. Dynamic assembly of FtsZ regulated by GTP hydrolysis. *EMBO J.* **17**, 462-469, (1998).

17 Gamba, P., Veening, J. W., Saunders, N. J., Hamoen, L. W. & Daniel, R. A. Two-step assembly dynamics of the *Bacillus subtilis* divisome. *J Bacteriol* **191**, 4186-4194, (2009).

18 Stokes, N. R. *et al.* Novel inhibitors of bacterial cytokinesis identified by a cell-based antibiotic screening assay. *J Biol Chem* **280**, 39709-39715, (2005).

## Figures legends

**Fig. 1: ADEP effects on polymerized FtsZ and FtsZ ring formation.**

**a**, Schematic of ADEP-dependent degradation of FtsZ. ADEP (orange) activates bacterial ClpP peptidase (blue) for untimely protein degradation, and nucleotide-free, monomeric FtsZ (dark green) represents a preferred protein substrate for ADEP-ClpP[12,14]. As a consequence, the cytoplasmic FtsZ pool is depleted (indicated by the shift from dark to light green), whereas GTP-bound FtsZ (GTP in yellow) is stabilized against proteolytic attack at antibiotic concentrations close to the MIC. FtsZ ring assembly relies on FtsZ treadmilling including the dynamic exchange of FtsZ subunits between the FtsZ ring and the cytoplasmic FtsZ pool (indicated by dark blue arrow). In the presence of ADEP, the depletion of the FtsZ pool results in an inhibition of FtsZ ring formation and cell division, finally leading to bacterial cell death. However, it remained unresolved, whether only early or also later stages of FtsZ ring formation are affected by ADEP treatment.

**b**, *In vitro* FtsZ polymerization and FtsZ degradation by ADEP-activated ClpP. Light transmission analyses of GTP-dependent FtsZ polymerization *in vitro* followed by incubation with a ClpP reaction mixture in the absence or presence of ADEP and/or GTP (-GTP/-ADEP, in grey; +GTP/-ADEP, in blue; +GTP/+ADEP, in orange). Here, polymerized FtsZ is not affected by incubation with ADEP-ClpP. As an independent control, we determined FtsZ protein amounts of samples that were incubated with or without GTP for 120 min in the absence or presence of ADEP. DMSO was used as an untreated control in all assays. The data shown is representative for at least two independent experiments, error bars indicate standard deviations. Representative SDS-PAGE images of triplicates are depicted.

**c,** Time-lapse fluorescence microscopy of exponentially growing *B. subtilis* 2020 cells treated with 0.125-0.25 µg/ml ADEP2. Overlaid fluorescence and phase contrast images show the localization of GFP-tagged FtsZ (in green) and the progression of FtsZ rings over time. The micrographs indicate that early FtsZ rings disintegrate during ADEP treatment (open triangles) while more

progressed FtsZ rings constrict and finish septum formation (closed triangles) to yield two separated daughter cells. Numbers indicate previously finished septa. For clarity, a phase contrast image of bacterial cells after 70 min of ADEP treatment is included at the end of the series to prove failure or success of septum formation. Overlay (5-40 min) or single channel (70 min) images are provided. Scale bar, 5 µm. Images are representative of at least three biological replicate cultures of *B. subtilis* 2020 with >600 FtsZ rings analyzed over time.

**d**, Super-resolution fluorescence microscopy of different stages of FtsZ ring formation in *B. subtilis* 2020. While all of the early stage FtsZ rings disintegrate upon ADEP treatment (100%, N=323), all late stage FtsZ rings further constrict and finalize septum formation (100%, N=140). Intermediate stage FtsZ rings, which were in transition from early to late stages, show a heterogenous behavior with 71% of FtsZ rings abrogating division and 29% further constricting and finalizing septum formation (N=178).

**e**, Time-lapse fluorescence microscopy of exponentially growing *B. subtilis* CM03 cells treated with 0.125-0.25 µg/ml ADEP2. Overlaid fluorescence and phase contrast images show the localization of mCherry-FtsZ or GFP-PBP2b, as indicated, during ADEP treatment over time. The micrographs indicate that the divisome consistently succeeds to finalize cell division (closed triangles) in the presence of ADEP in situations when PBP2b is substantially detected at the septum area. In contrast, earlier stage FtsZ rings, prior to the visible arrival of PBP2b at the septum, disintegrate during ADEP treatment (open triangles). For clarity, a phase contrast image of bacterial cells after 99 min of ADEP treatment is included at the end of the series to prove failure or success of septum formation. Overlay (0-45 min) or single channel (99 min) images are provided. Scale bar, 5 µm. Images are representative of at least three biological replicate cultures of *B. subtilis* CM03 with >200 septa/FtsZ rings analyzed over time.

**Fig. 2: Proposed two-step model of FtsZ ring constriction during cell division in *B. subtilis*.** At antibiotic concentrations close to the MIC, ADEP treatment essentially depletes the cytoplasmic pool of nucleotide-free FtsZ[14], thereby continuously sequestering available FtsZ that is needed for FtsZ ring formation and treadmilling[9,10]. Our data reveal that ADEP-treatment leads to the disintegration of early FtsZ rings (framed green) in *B. subtilis*, while more progressed FtsZ rings (framed red) resisted degradation and finished septum formation as well as daughter cell separation, suggesting distinct stages during FtsZ ring initiation, progression and maturation. Therefore, we propose a two-step model of FtsZ ring constriction in *B. subtilis*. In the initial stages, FtsZ ring formation essentially relies on FtsZ treadmilling, indicated by the disintegration of early FtsZ rings upon ADEP-dependent depletion of the cytoplasmic FtsZ pool. In the later stages, more progressed FtsZ rings are significantly less sensitive to a depletion of the cytoplasmic FtsZ pool, implying that other triggers than treadmilling FtsZ proteins take over to drive divisome constriction, for example, peptidoglycan synthases that arrive at the divisome during the later stages of cell division.

## Figures

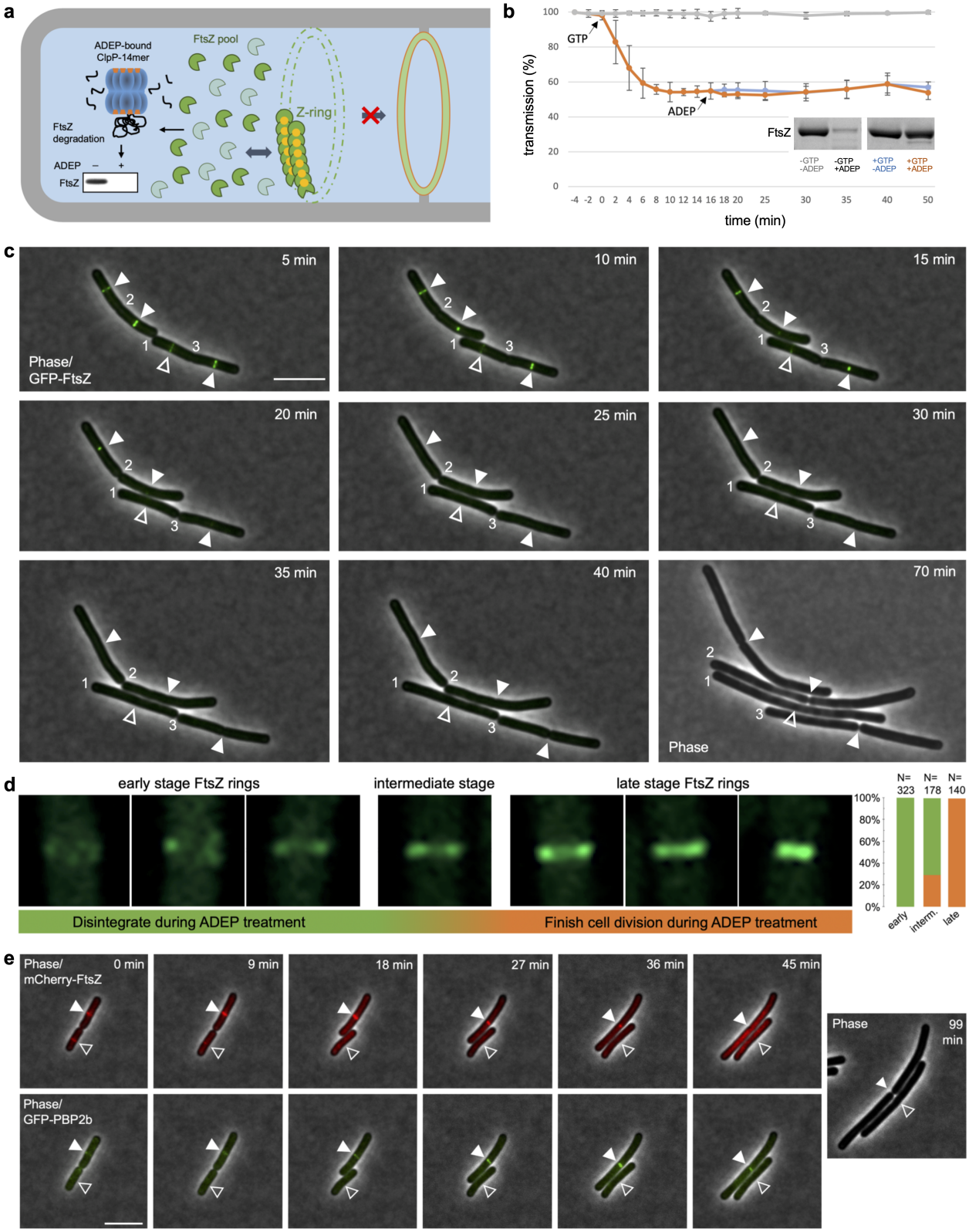


Figure 1

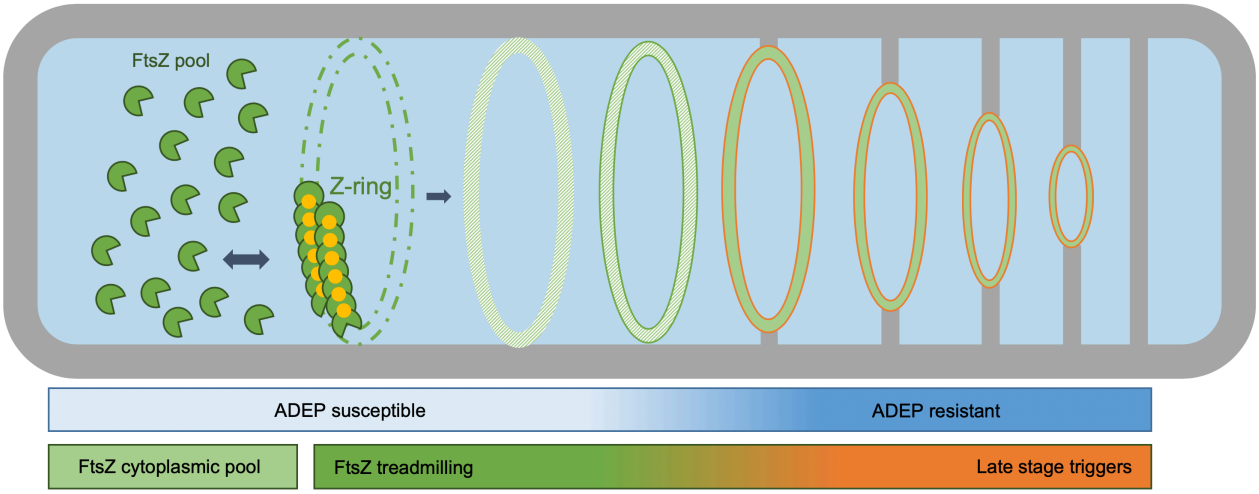
FtsZ pool
Z-ring
ADEP susceptible
ADEP resistant
FtsZ cytoplasmic pool
FtsZ treadmilling
Late stage triggers

Figure 2

## Supplementary information

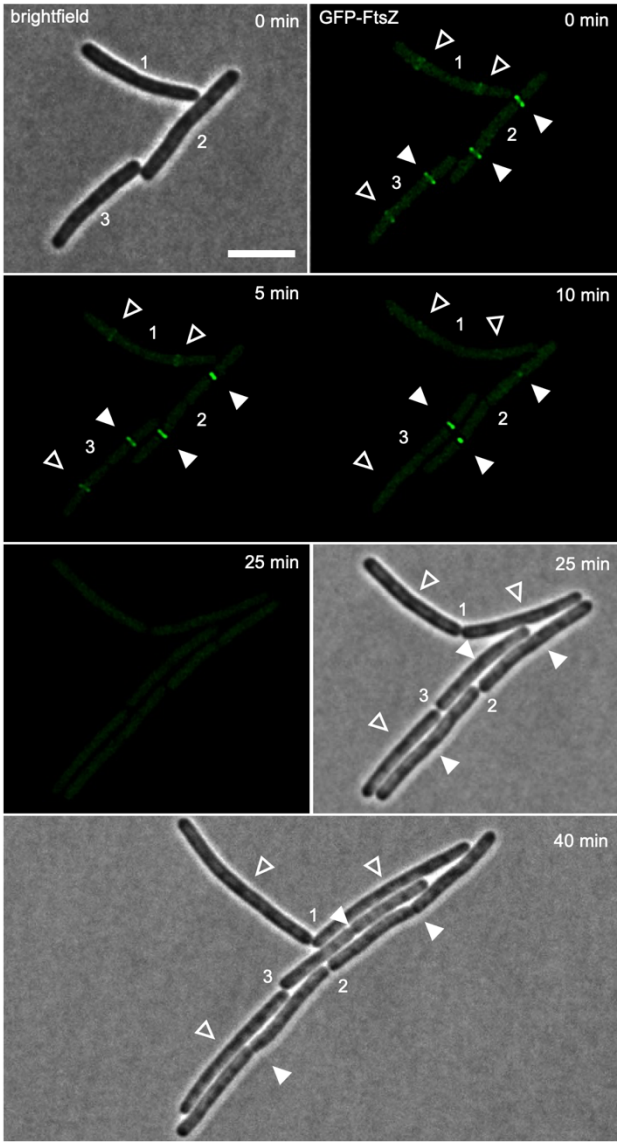


Fig. S1: ADEP-treatment leads to the disintegration of early, but not late stage FtsZ rings. Super-resolution fluorescence microscopy of exponentially growing *B. subtilis* 2020 cells treated with 0.25 µg/ml ADEP2. Fluorescence images show the localization of GFP-tagged FtsZ and the progression of FtsZ rings (in green) over time. During ADEP treatment, early FtsZ rings disintegrate (open triangles), while mature FtsZ rings finish septum formation (closed triangles). Numbers indicate already finished, but undivided septa. Scale bar, 5 µm. Images are representative of at least three biological replicate cultures.

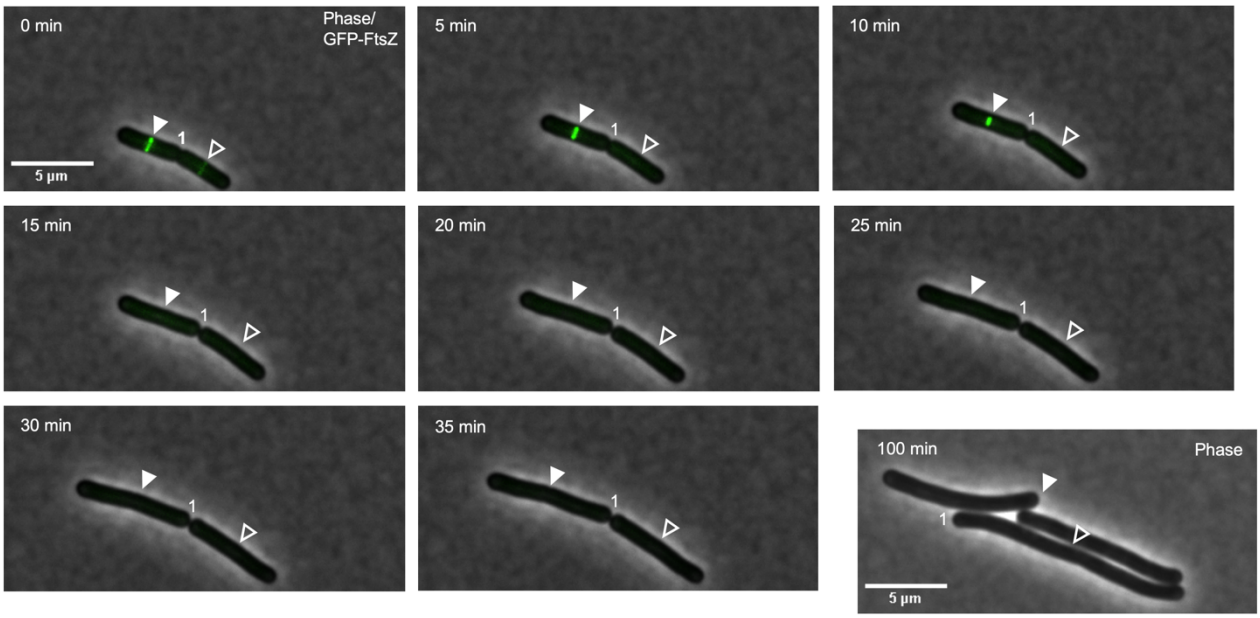


Fig. S2: Effect of ADEP treatment on FtsZ ring formation in *B. subtilis* cells visualized by time-lapse fluorescence microscopy.

Exponentially growing *B. subtilis* 2020 cells were treated with ADEP2 and FtsZ ring formation was followed over time. Micrographs show overlays of phase contrast images (greyscale) and GFP fluorescence images (green) indicating FtsZ ring formation at mid-cell. ADEP-treated cells show disintegration of early FtsZ rings (open triangles) while progressed FtsZ rings constrict and finalize septum formation to yield two separated daughter cells (closed triangles). Numbers indicate already finished, but undivided septa. For clarity, numbers remain positioned to the corresponding cell pole of the daughter cell on the right. An additional phase contrast image was acquired after prolonged incubation with ADEP (last image in the series) indicating failure or success of septum formation. Scale bars, 5 µm. Images are representative of at least three biological replicate cultures of *B. subtilis* with >600 FtsZ rings analyzed over time.

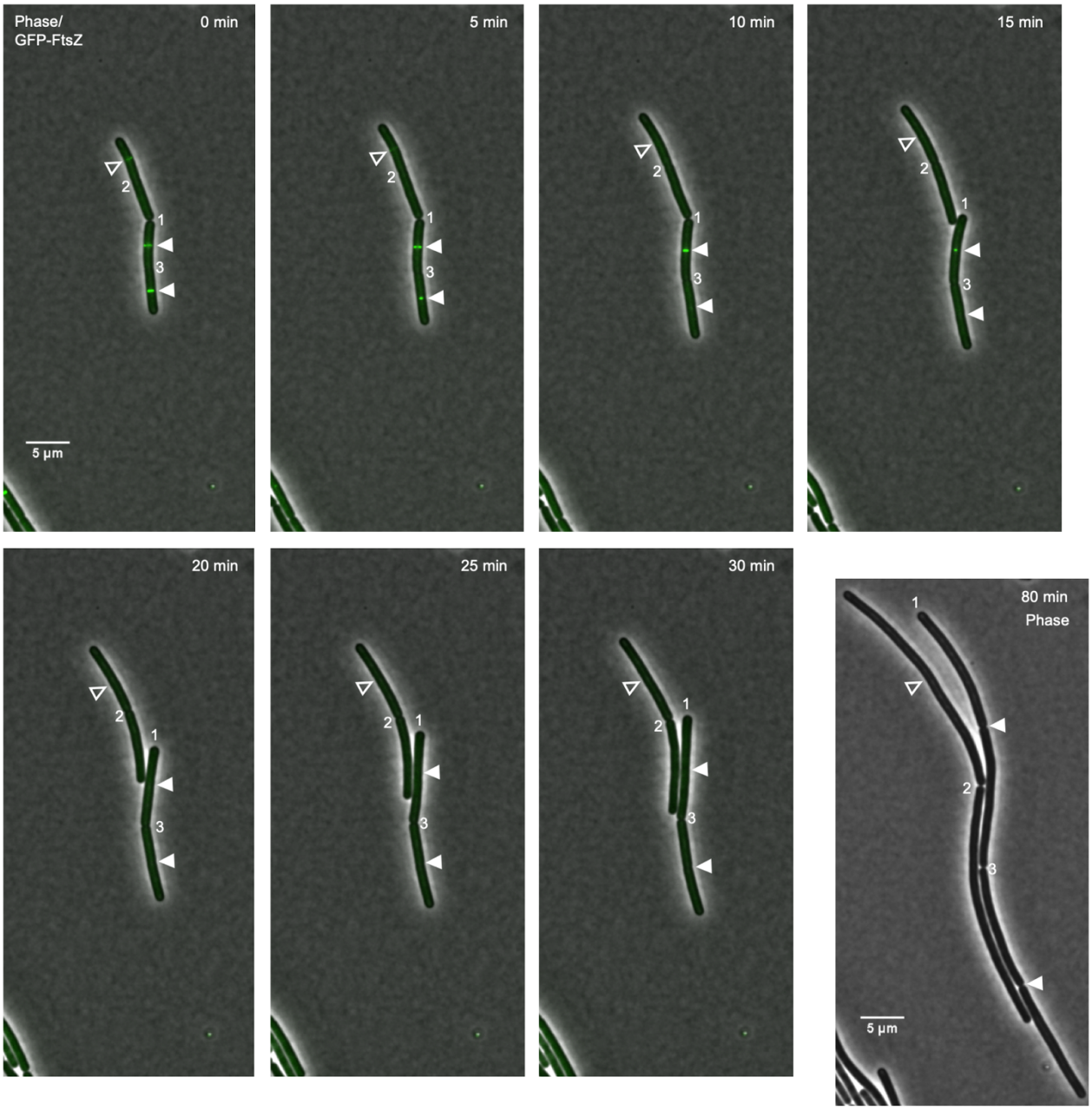


Fig. S2 continued: Effect of ADEP treatment on FtsZ ring formation in *B. subtilis* cells visualized by time-lapse fluorescence microscopy.

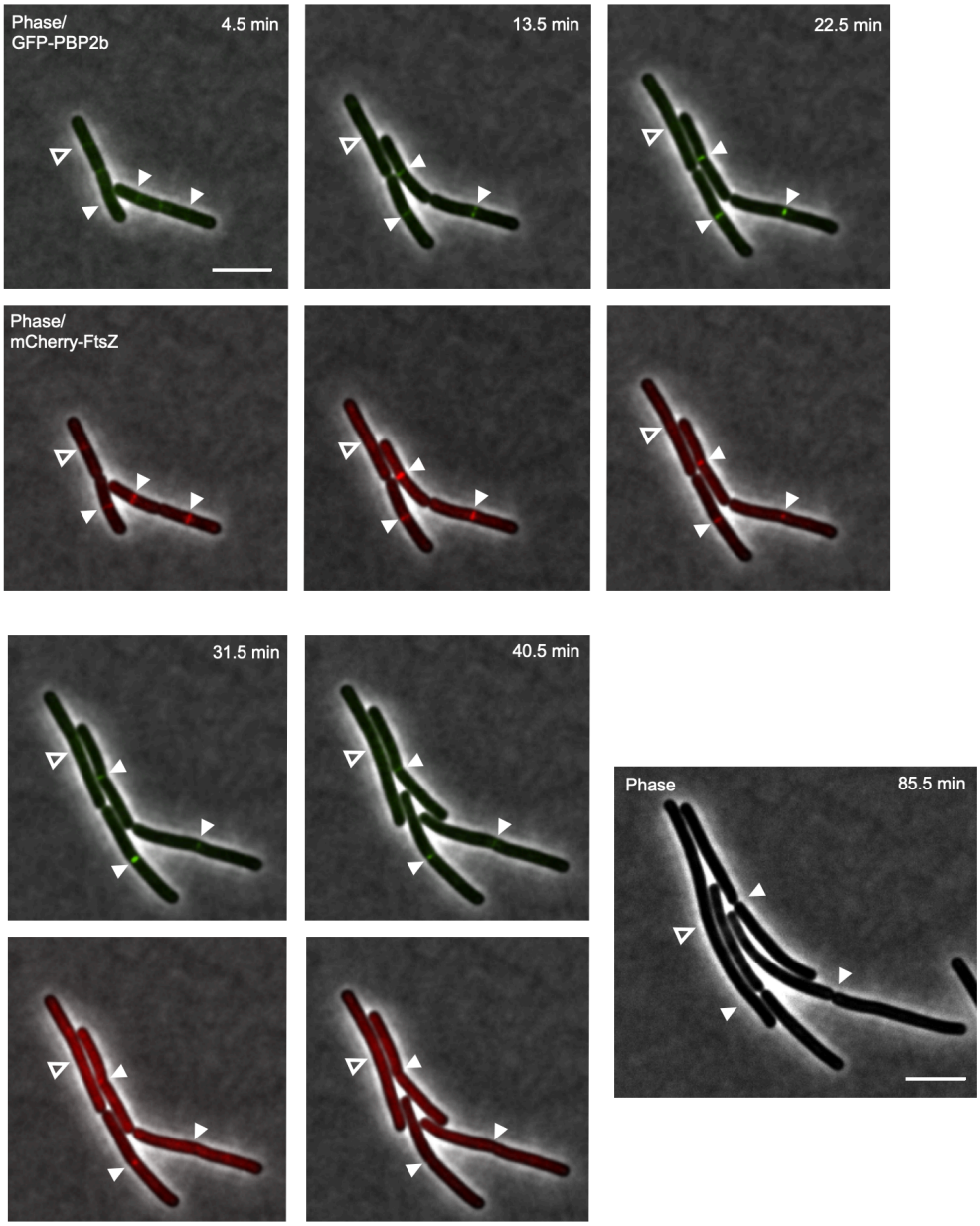


Fig. S3: Colocalization studies of mCherry-FtsZ and GFP-PBP2b during ADEP treatment of *B. subtilis* cells visualized by time-lapse fluorescence microscopy.

Overlaid fluorescence and phase contrast images are shown. During ADEP treatment, early FtsZ rings disintegrate (open triangles), while mature FtsZ rings finish septum formation once PBP2b has substantially arrived at the septum (closed triangles). A phase contrast image of bacterial cells after 85.5 min of ADEP treatment is included at the end of the series to prove failure or success of septum formation. Scale bars, 5 µm. Images are representative of at least three biological replicate cultures of *B. subtilis* with >200 FtsZ rings analyzed over time.